Numerical Study of the Capability of Various Turbulence Models to Predict the Heat Transfer Characteristics of Supercritical Water Flow

P J Saji[1], S Suresh[2], R Dhanuskodi[3], P Mallikarjuna Rao[4], D Santhosh Kumar[5]
[1,2,4]*Department of Mechanical Engineering,National Institute of Technology, Tiruchirappalli-620015, India.*
[3,5]*Research and Development Department,Bharat Heavy Electricals Limited, Tiruchirappalli-600014, India.*

ABSTRACT

A two-dimensional model is developed to numerically study the capability of various turbulence models to predict the heat transfer characteristics of supercritical water flowing through a vertical tube. At the tube inlet, mass flux of 1260 kg/m^{2}s is applied. At the tube outlet, normal gradients of velocity, Turbulence Kinetic energy and Turbulence dissipation rate (k and ε) are assigned zero and a pressure of 245.2 bar is specified. Uniform heat flux condition ranging from 233 to 698 kW/m^2 is applied around the tube wall. After performing a grid independence test, a non-uniform mesh of 200 nodes along the radial direction and 600 uniform nodes along the axial direction was chosen. To capture the large variations of flow field variables near the tube wall, a fine grid is used close to the wall (wall y+ <0.3).A set of standard two equation models (Standard k-ε, RNG k-ε, k-ω SST)and 5 Low Reynolds Number (Low Re) models are chosen in the present study. The results are compared with the experimental results of Yamagata *et al*. (1972). The tube wall temperature was plotted as a function of the fluid enthalpy. It is seen that under moderate heat flux conditions, the average difference between the wall temperature prediction by various models and the experimental results are within 3 °C. Standard k-ε, RNG k-ε and Two Low Re models came closest to the experimental results under the given conditions. Considering the computational time taken, RNG k-ε model has been picked as the best choice. The model is also validated for its capability to work at higher heat fluxes.

KEYWORDS: Supercritical water, Turbulence modeling, Tube wall temperature prediction, Heat transfer characteristics

NOMENCLATURE

G	mass flux [kg/(m^{2}s)]
k	turbulence kinetic energy [m^2/s^2]
q	heat flux [kW/m^2]
T	temperature [°C]
u	velocity component [m/s]
p	pressure [bar]
y+	dimensionless wall function
ε	turbulence dissipation rate [m^2/s^2]
τ	turbulence stress [N/m^2]
ω	Inverse turbulence time scale

Abbreviations

RANS	Reynolds averaged Navier-Stokes
SST	Shear Stress Transport
SIMPLE	Semi-implicit method for pressure linked equations
QUICK	Quadratic upstream interpolation of convective kinematics

I. INTRODUCTION

Due to the acute variation in the thermo-physical properties of supercritical fluids (Figure 1) near their pseudo critical point, they are being used in a wide range of engineering applications such as thermal power generation, nuclear power generation, refrigeration applications, electronic applications, chemical applications, pharmaceutical applications etc. Most of the applications make use of the higher specific heat near the pseudo critical region.Even though research in supercritical applications started as early as 1930, the idea of using the same in thermal power generation was unleashed in the 1950's. 50's saw a series of pilot scale plants being set up in US and USSR. Improvement in overall unit efficiency at higher pressures was the driving point behind this trend. At higher turbine inlet pressure, the net mechanical energy available from the Rankine cycle increases compared to that from subcritical pressure. This is due to the improvement in the quality of energy at higher pressures, in other words it is due to the decrease in irreversibilities associated with energy conversion at higher pressures.

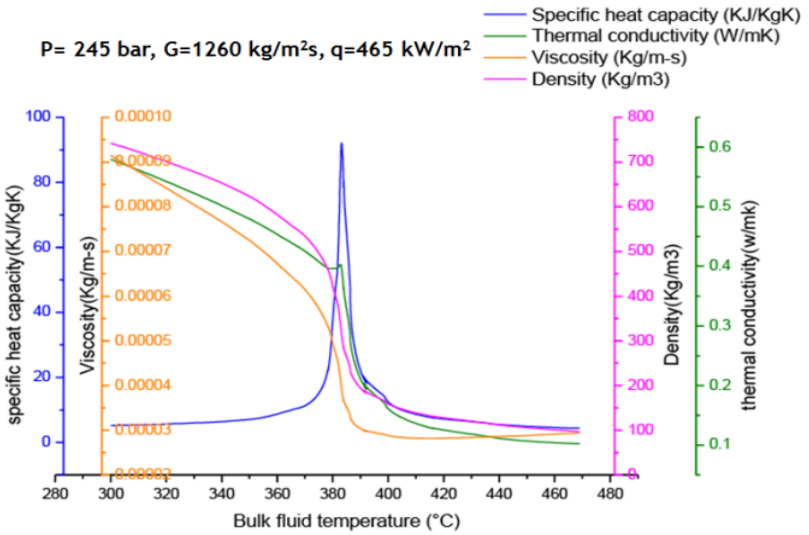

Figure 1. Variation of properties near pseudo critical point

The efficiency of a standard subcritical power plant is in the range 36-38% while that of a supercritical plant is above 42% and for ultra-supercritical and advanced ultra-supercritical plants, the value is above 46%.The increase in pressure to improve efficiency was the only scope of improvement left out in the Rankine cycle as for other limits, no further pushing was possible nor they were economical. The ever increasing quest for efficiency improvement has seen more power plants being designed and operated at higher pressures. The initial sluggishness in the commercial scale development of the supercritical plants was overcome by the development of higher grade austenitic steels. By late 80's, several supercritical power plants were engineered and started commercial operation with superheated steam conditions as high as 600°C and 300 bar. Research in this area started picking up in Asia by the early 21st century. China was the front-runner among the Asian countries followed by India. Because of the advantages like higher unit efficiency, lower pollutant emission and lower fuel consumption, supercritical boilers outperform the subcritical power plants. The difficulty in meeting the fuel supply to demand and the awareness of global climate shift has made this cleaner technology more acceptable among developing countries like India.

It is found that the temperature of the fluid (water) in the evaporator region of the present supercritical boilers is roughly in the range of 350° to 450°C, within which the pseudo critical temperature of 384.7 ^{o}C at 250 bar is likely to occur. In the vicinity of the pseudo critical point, strong variations in properties combined with a high heat flux can lead to a Deteriorated Heat Transfer (DHT). Even though this phenomenon is not as severe as the similar phenomenon in subcritical range namely Departure from Nucleate Boiling (DNB), it can cause appreciable decrease in the heat transfer coefficient and hence increase in the wall temperature. Under extreme conditions, the temperature can exceed the metal oxidation limit and the tube can fail. Therefore, it is indeed necessary to study the heat transfer behavior of water at supercritical conditions and the influence of the same on wall temperature. Since the turbulence modelling is highly influenced by the large variation in fluid properties at supercritical conditions, mathematical modelling is an uphill task. The turbulence model suitable for a certain range of operation may not give similar results under other conditions.

That is, a model which predicts well the heat transfer deterioration may not predict the heat transfer deterioration well. So it is important to understand various models and how they behave under various conditions. A set of standard two equation models (Standard *k-ε*, RNG *k-ε*, *k-ω* SST) and 5 Low Reynolds Number (Low Re) models are chosen in the present study for evaluation using experimental results of Yamagata *et al.* (1972).

II. NUMERICAL METHOD

2.1 Turbulence models

Turbulence flows are high Reynolds number flows which are chaotic or random in nature. The flow field parameters of a turbulent flow are highly unpredictable and a fully deterministic or analytical solution is difficult since the parameters cannot be expressed quantitatively with accuracy. So turbulent flows are described statistically. The unsteady nature of the parameters (velocity, temperature and pressure) assists in the transfer of matter, momentum and energy between fluid particles. The diffusivity of turbulence causes rapid mixing and increased rates of momentum, heat, and mass transfer. A flow that looks random but does not exhibit the spreading of velocity fluctuations through the surrounding fluid is not turbulent.The velocity and pressure components are decomposed into the sum of a mean component and a fluctuating component. The mean component can be time average or space average, but mostly time average. The resultant equations are called the Reynolds Averaged Navier Stokes (RANS) equations.

Expressing as the sum of mean and fluctuating component,

$$n_i = \bar{n}_i + \acute{n}_i \tag{1}$$

where n_i is the specific property which can be velocity, temperature or density,
$\bar{n}_i$ is the time average component and $\acute{n}_i$ is the turbulence fluctuating component

Thus the process of averaging has introduced a new term (product of fluctuating components) known as the Reynolds stress or turbulent stress. As a result of this there are six additional unknowns in the RANS equations. The main task of turbulence modelling is to develop computational procedures of sufficient accuracy to accurately predict the Reynolds stresses and the scalar transport terms. This will then allow for the computation of the time averaged flow and scalar fields without having to calculate the actual flow fields over long time periods. This process is called closure of the model.The additional turbulent stress term in the RANS is predicted with required accuracy in a number ways. Two equation models are the most widely used models due to their simplicity. These models provide expression for computation of kinetic energy *k* and for the turbulence length scale or equivalent. Apart from the standard two equation models, there are Low Reynolds number models which consider viscous damping functions in the viscous sub layer where the Reynolds number is quite low. They are modified *k-ε* models.

2.2 Governing Equations

As in any numerical code for flow dynamics and heat transfer, the governing equations are simply versions of the conservation laws of classic physics-

2.2.1 Conservation of Mass (Continuity Equation): For incompressible flow, continuity equation for the mean component can be written as

$$\frac{\partial \bar{u}_j}{\partial x_j} = 0 \tag{2}$$

2.2.2 Conservation of Momentum: The general form of momentum equation can be written as

$$\rho\left[\frac{\partial \bar{u}_i}{\partial t} + \frac{\partial\left(\bar{u}_i \bar{u}_j\right)}{\partial x_j}\right] = -\frac{\partial \bar{p}}{\partial x_i} + \frac{\partial\left(\mu \frac{\partial \bar{u}_i}{\partial x_j}\right)}{\partial x_j} - \frac{\partial\left(\rho \overline{\acute{u}_i \acute{u}_j}\right)}{\partial x_j} \tag{3}$$

2.2.3 Conservation of Energy: The general form of energy equation can be written as

$$\rho\frac{\partial k}{\partial t} + \rho\bar{u}_j\frac{\partial k}{\partial x_j} = -\tau_{ij}\frac{\partial \bar{u}_i}{\partial x_j} - \rho\epsilon + \frac{\partial\left[\left(\mu + \frac{\mu_T}{\sigma_k}\right)\frac{\partial k}{\partial x_j}\right]}{\partial x_j} \tag{4}$$

where τ_{ij} is the turbulence stress tensor, ϵ is the dissipation rate of k.

2.3 Physical Model

In the present work, a two-dimensional axisymmetric model is developed to numerically study the heat transfer characteristic of supercritical water flowing through a vertical tube with uniform heating and the effect of diameter on heat transfer has been analysed. A 7.5 mm diameter tube is used for analysis. Length of the tube

is varied from case to case to obtain the required outlet temperature. In order to obtain a fully developed flow, the modelled tube is extended at the inlet by 0.5m. The physical model is depicted in Figure 2.

For the calculation of the thermodynamic properties of supercritical fluids, the NIST database available in FLUENT is used. The SIMPLE algorithm is used to simultaneously solve the velocity and pressure equations. The QUICK scheme is used to approximate the flow field variables in the discretized convective terms in transport equations.

.

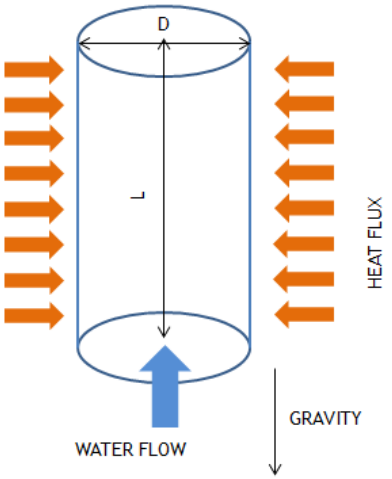

Figure 2. Schematic representation of the tube geometry

2.4 Grid Independence Test

The selection of grid is important since the accuracy of the results depends on the fineness of the grid. On the other side, beyond a certain point, further refinement of grid will not improve the solution; rather it will turn out to be wastage of computational time. Here, a grid independence test has been conducted to choose an appropriate mesh for the above physical model. Grids with 100 x 600, 120 x 600, 140 x 600, 175 x 600 and 200 x 600 (radial nodes x axial nodes) were tested. Non-uniform nodes with a successive ratio of 1.025 in the radial direction and uniform nodes in the axial direction have been used for all the grids.In order to evaluate the accuracy of the test results, the experimental data of Yamagata et al. (1972) has been selected for validation. A 7.5 mm diameter tube is used with a heat flux of 465 kW/m^2 and mass flux of 1260 kg/m^2. Operating pressure was 245 bar. The comparison is plotted in Figure 3. It can be seen that 200 x 600 grids matches well with that of experiment data. Further increase in grids does not improve the accuracy of the solution.

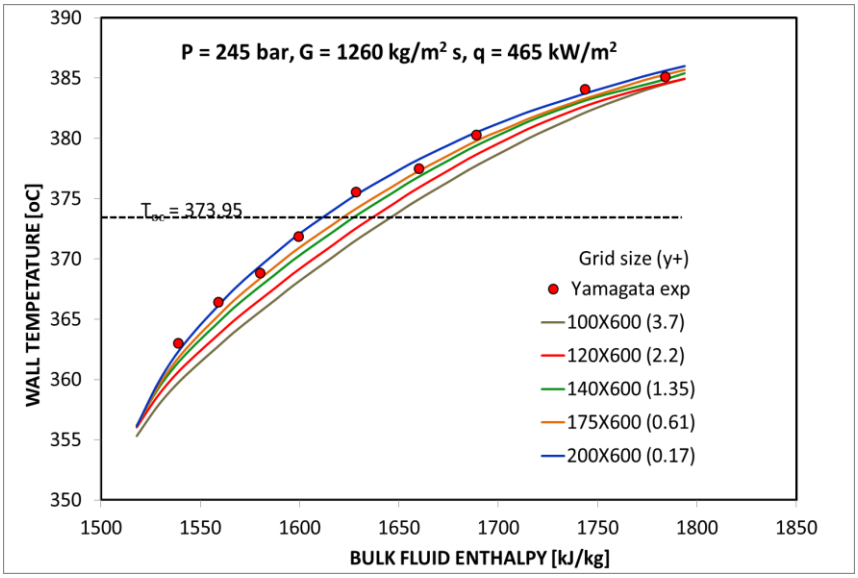

Figure 3. Grid Independence test

III. RESULTS AND DISCUSSION

3.1 Model comparison

Eight two equation models available in the FLUENT are chosen for heat transfer prediction capability study in the present case. Standard two equation turbulence models such as standard *k-ε*, RNG *k-ε* model with enhanced wall treatment and *k-ω* SST are chosen. Five low Reynolds number models namely models by Abid, Lam-Bremhost, Launder-Sharma, Yang-Shih and Chang-Hsieh-Chen are also selected. A 7.5 m tube is used with an inlet mass flux of 1260 kg/m^2 and heat flux of 233 kW/m^2 has been used. The heat flux to mass flux ratio is less in this case and normal heat transfer is expected throughout the operation range with an improvement in heat transfer near the pseudo critical region.For comparing the heat transfer prediction capability of the models, the plot of tube wall temperature vs. the bulk fluid enthalpy is chosen. This is a good tool for analysis since it can be inferred from the plot that the region under consideration favours heat transfer enhancement or deterioration. A decrease in the slope of the wall temperature curve depicts an improvement in heat transfer and an increase in slope indicates the other way around. The wall temperature plot is compared with the experimental result of Yamagata et al. (1972) under same conditions for all eight models selected for evaluation.

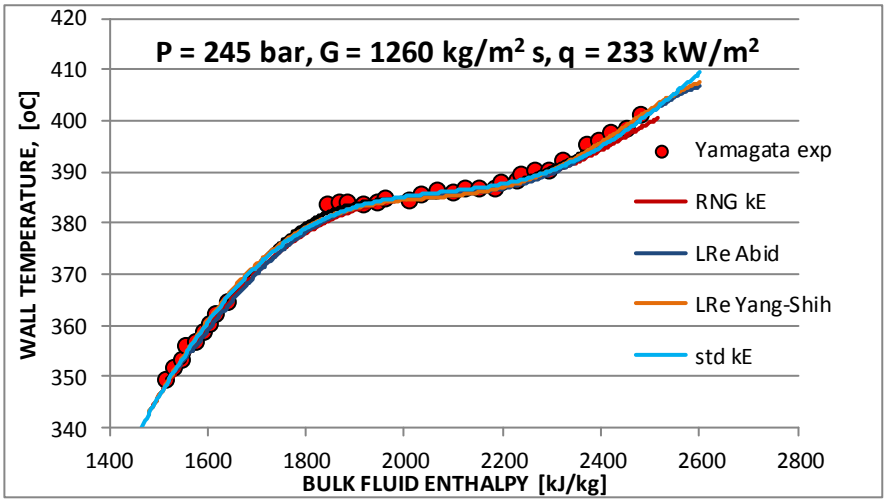

Figure 4. Models predicting the wall temperature closely

It is seen that four out of eight models considered are closely following the experimental results as seen in Figure 4. The average difference between the wall temperature between these models and the experimental data is less than 1°C. For better clarity, a portion of the above plot is expanded to have a closer look (Figure 5). A region close to pseudo critical region is selected since the property variations are maximum in this region. Due to the property variation, the deviation from the experimental data is expected to be a maximum in this region. So the capability of the models to predict the heat transfer characteristics in the above region is particularly checked.

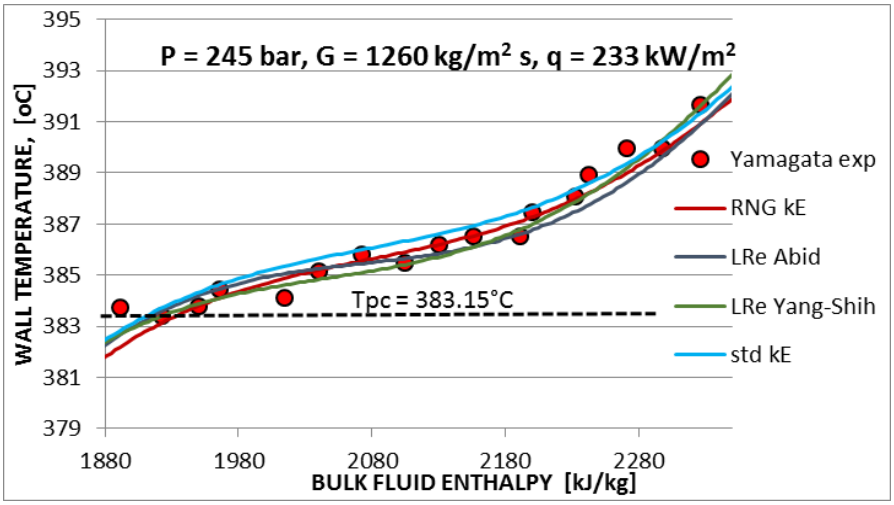

Figure 5. Expanded view of models predicting the wall temperature closely

It is seen that the RNG *k-ε* model and the Low Reynolds number model by Abid are the closest to experimental results. The average differences calculated between the wall temperature prediction by these models and the experimental wall temperature are 0.3°C and 0.4°C respectively. It can be seen that the wall temperatures of all the models follow similar trend. When the bulk enthalpy is less than 1900 kJ/kg, the wall temperature ascends linearly following enthalpy increase. The wall temperature curves become flat between 1900 kJ/kg and 2200 kJ/kg. This is because the region covers the pseudo critical zone where the specific heat is substantially higher than the normal value. The specific heat increases from the normal value of 4.18 kJ/kg-K and assumes a value as high as few tens (90 kJ/kg-K) as seen in Figure 1. This enhances the heat transfer coefficient and the fluid enthalpy increases without notable increase in the wall temperature. The wall temperature increases again beyond 2200 kJ/kg where specific heat falls down. So it can be said that the above 4 models are working well in the supercritical region under the heat transfer enhancement region.

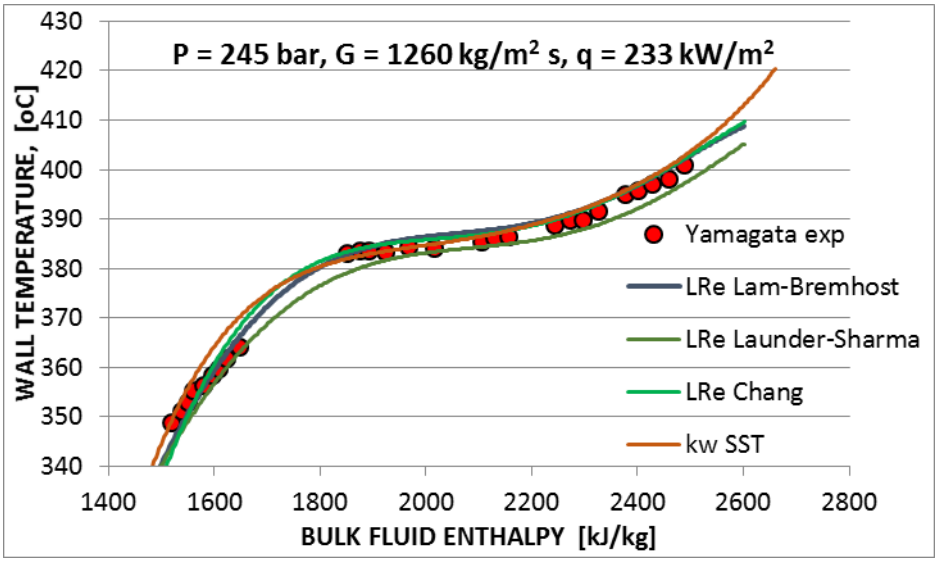

Figure 6.Wall temperature prediction by models

The wall temperature plots for the other four models are slightly offset from the experimental data with the average difference between the prediction and experimental wall temperature ranging from 1.1 °C to2.7 °C. The wall temperature plots are depicted in Figure 6.The average difference between the wall temperature prediction by the models and the experimental wall temperature is tabulated in Table 1 below

Table 1. Average difference between model prediction and experimental data

Sl no	Model	Average difference in temperature [°C]
1	RNG *k-ε* model with enhanced wall treatment	0.3
2	Low Re model by Abid	0.4
3	Low Re model by Yang-Shih	0.5
4	Standard *k-ε* model	0.5
5	*k-ω* SST model	1.1
6	Low Re model by Lam-Bremhost	1.7
7	Low Re model by Chang-Hseih-Chen	1.9
8	Low Re model by Launder-Sharma	2.7

It is seen that first four models (RNG *k-ε* model with enhanced wall treatment, Low Re model by Abid, Low Re model by Yang-Shih, Standard *k-ε* model) are predicting closely the wall temperature compared to the experimental data. The average temperature difference is within 1 °C. The latter four models (*k-ω* SST model, Low Re model by Lam-Bremhost, Low Re model by Chang-Hseih-Chen, Low Re model by Launder-Sharma) are showing higher deviations up to 2.7°C.

Computation time is also considered in the model selection. Low Re models are more time consuming compared to the standard models. They take approximately 20% more time than the standard model. So considering the accuracy of prediction and the computational time, RNG *k-ε* model with enhanced wall treatment is the best model under the conditions considered.

3.2 Validation

The heat flux considered in the above tests was 233 kW/m^2. The above study was extended to a higher heat flux (698 kW/m$^{2)}$ to ascertain the capability of selected RNG *k-ε* model at higher ranges. The wall temperature prediction is compared with the experimental data of Yamagata et. al (1972) under the same conditions. The plot is shown in Figure 7. It is seen that at higher heat flux also the model is predicting well. The average temperature difference between prediction and experiment data is within 0.5°C.

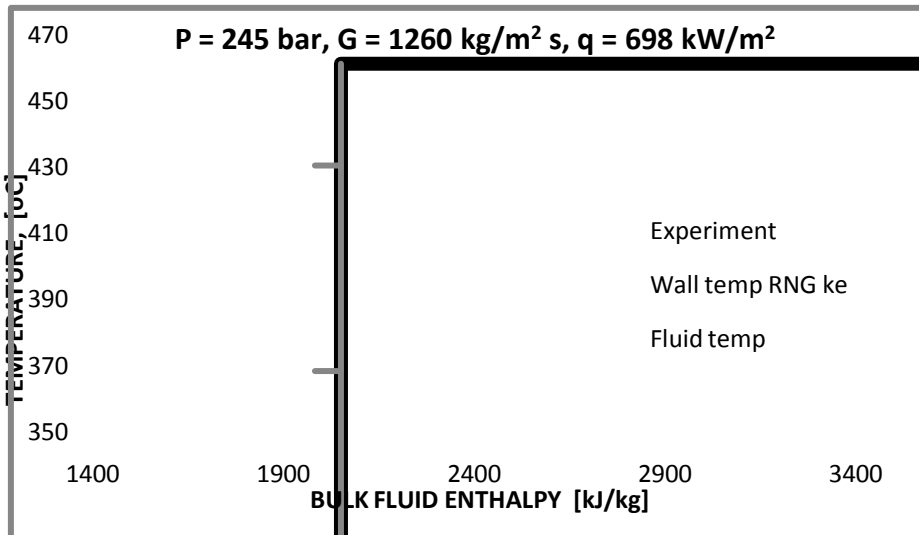

Figure 7.Wall temperature prediction by RNG k-ε model with EWT

IV. CONCLUSION

- For the selected case, the standard two equation models such as standard *k-ε*, RNG *k-ε* model with enhanced wall treatment and *k-ω* SST models are in good agreement with the experimental results under supercritical conditions with low heat flux to mass flux ratios.
- Low Re models such as models by Abid, Lam-Bremhost, Launder-Sharma, Yang-Shih and Chang-Hsieh-Chen also work well under the same conditions.
- Under low heat flux to mass flux ratios the maximum difference between the predicted wall temperature and experimental data is 2.7 °C for the model by Launder-Sharma which is the maximum deviation.
- RNG *k-ε* model with enhanced wall treatment is the best among the compared models with respect to the accuracy and the computational time. The average temperature difference for this model is 0.3°C.
- RNG *k-ε* model with enhanced wall treatment works well at moderately high heat flux of 698 kW/m^2 and for an enthalpy range 1450kJ/kg to 2750 kJ/kg.

REFERENCES

[1] K Yamagata, K Nishikawa, S Hasegawa, I Fuji and S Yoshida. Forced Convective Heat Transfer to Supercritical Water Flowing in Tubes, Int. J. Heat Mass Transfer,15, pp. 2575-2593. 1972

[2] Medhat Sharabi and Walter Ambrosini. Discussion of heat transfer phenomena in fluids at supercritical pressure with the aid of CFD models, Annals of Nuclear Energy,36, pp. 60–71, 2009

[3] Pioro I.L., Duffey R.B. Experimental heat transfer in supercritical water flowing inside channels (survey). Nucl. Eng. Des. 235, 2407–2430, 2005

[4] Incropera F.P., DeWitt D.P., Bergman Th.L., Lavine A.S. Fundamentals of Heat and Mass Transfer, 6th edition. J. Wiley & Sons, New York, NY, USA, 2007

[5] NIST Reference Fluid Thermodynamic and Transport Properties. REFPROP, NIST Standard Reference Database 23 (on diskette: Executable with Source), Ver. 7.0, E.W. Lemmon, M.O. McLinden, M.L. Huber, U.S. Dept. of Commerce, 2002

[6] Xiaojing Zhu, Qincheng Bi, Dong Yang, Tingkuan Chen. An investigation on heat transfer characteristics of different pressure steam-water in vertical upward tube, Nuclear Engineering and Design 239, pp. 381–388, 2009